



HAL
open science

Effects of a New Natural Catechol-O-methyl Transferase Inhibitor on Two In Vivo Models of Parkinson's Disease

Valeria Parrales-Macias, Abha Harfouche, Laurent Ferrié, Stéphane Haïk, Patrick Michel, Rita Raisman-Vozari, Bruno Figadère, Nicolas Bizat, Alexandre Maciuk

► To cite this version:

Valeria Parrales-Macias, Abha Harfouche, Laurent Ferrié, Stéphane Haïk, Patrick Michel, et al.. Effects of a New Natural Catechol-O-methyl Transferase Inhibitor on Two In Vivo Models of Parkinson's Disease. ACS Chemical Neuroscience, 2022, 13 (23), pp.3303-3313. 10.1021/acscchemneuro.2c00356 . hal-04869527

HAL Id: hal-04869527

<https://hal.science/hal-04869527v1>

Submitted on 7 Jan 2025

HAL is a multi-disciplinary open access archive for the deposit and dissemination of scientific research documents, whether they are published or not. The documents may come from teaching and research institutions in France or abroad, or from public or private research centers.

L'archive ouverte pluridisciplinaire **HAL**, est destinée au dépôt et à la diffusion de documents scientifiques de niveau recherche, publiés ou non, émanant des établissements d'enseignement et de recherche français ou étrangers, des laboratoires publics ou privés.



Distributed under a Creative Commons Attribution - NonCommercial - NoDerivatives 4.0 International License

Effects of a new natural catechol-O-methyl transferase inhibitor on two *in vivo* models of Parkinson's disease

Valeria Parrales-Macias[¶], Abha Harfouche[¶], Laurent Ferrié, Stéphane Haïk, Patrick P. Michel, Rita Raisman-Vozari, Bruno Figadère, Nicolas Bizat*, Alexandre Maciuk*

Valeria Parrales-Macias - ICM, Hôpital Pitié Salpêtrière, Paris, 75013, France

Abha Harfouche - Université Paris-Saclay, CNRS, BioCIS, Orsay, 91400, France

Laurent Ferrié - Université Paris-Saclay, CNRS, BioCIS, Orsay, 91400, France

Stéphane Haïk - ICM, Hôpital Pitié Salpêtrière, Paris, 75013, France

Patrick P. Michel - ICM, Hôpital Pitié Salpêtrière, Paris, 75013, France.

Rita Raisman-Vozari - ICM, Hôpital Pitié Salpêtrière, Paris, 75013, France

Bruno Figadère – Université Paris-Saclay, CNRS, BioCIS, Orsay, 91400, France

Nicolas Bizat – ICM, Hôpital Pitié Salpêtrière, Université de Paris Cité, Paris, 75013, France

*nicolas.bizat@icm-institute.org

Alexandre Maciuk – Université Paris-Saclay, CNRS, BioCIS, Orsay, 91400, France

*alexandre.maciuk@universite-paris-saclay.fr

¶These authors contributed equally to the work.

ABSTRACT: A tetrahydroisoquinoline identified in *Mucuna pruriens* ((1*R*,3*S*)-6,7-dihydroxy-1-methyl-1,2,3,4-tetrahydroisoquinoline-1,3-dicarboxylic acid, compound **4**) was synthesized and assessed for its *in vitro* and *in vivo* pharmacological profile on two animal models of Parkinson's disease. Compound **4** inhibits catechol-O-methyltransferase (COMT) with no affinity for the dopaminergic receptors or the dopamine transporters. It restores dopamine-mediated motor behavior when it is co-administered with L-DOPA to *C. elegans* animals with MPP+ damaged dopaminergic pathway. In a 6-OHDA rat model of Parkinson's disease, its co-administration at 30 mg/kg with L-DOPA enhances the effect of L-DOPA with an intensity similar to tolcapone **1** at 30 mg/kg but for a shorter duration. The effect is not dose-dependant. Compound **4** seems not to cross blood-brain barrier and thus acts as a peripheral COMT inhibitor. The COMT inhibition showed by compound **4** further validates the traditional use of *M. pruriens* for the treatment of Parkinson's disease, and compound **4** can thus be considered as a promising drug candidate for the development of safe, peripheral COMT inhibitors.

KEYWORDS: Parkinson's disease; catechol-O-methyltransferase; *Mucuna pruriens*; *Caenorhabditis elegans*; dopaminergic pathway; animal models.

INTRODUCTION

Parkinson's disease (PD) is a neurodegenerative disorder characterized by the extenuation of dopaminergic neurons in the *substantia nigra pars compacta* (SNc) associated with a loss of striatal dopamine. The resulting disruption of neurotransmitter signaling is responsible for most symptoms of PD. Levodopa (L-DOPA), the natural dopamine precursor, was introduced in the late 1960s as drug treatment and since then, has remained the most efficient chemotherapy for PD, in co-administration with a peripheral aromatic amino acid decarboxylase inhibitor (AADCi) aimed at blocking the peripheral formation of dopamine (Figure 1). Nevertheless, long-term use of L-DOPA/AADCi can end up with the administration of up to 8 g/day of L-DOPA and after some years of stable benefits, it consistently leads to wearing-off, where the clinical response diminishes and new side-effects develop, including dyskinesia and on-off periods¹. Several hypotheses tend to explain this phenomenon, in which L-DOPA and its metabolites play a key role^{1,2,3,4}. Besides being transformed into dopamine by AADC, L-DOPA can also be metabolized by COMT into 3-OMD (Figure 1). 3-OMD has been shown to induce several deleterious effects suggesting its role in the side effects of long-term L-DOPA treatment⁵. Thus, the combination of a COMT inhibitor (COMTI) with the L-DOPA/AADCi therapy is a common clinical practice to reduce the administered doses of L-DOPA, extend its serum concentration and decrease its side effects, hence a longer and better clinical response.

Potent and selective COMTIs bearing a nitrocatechol (= 3-nitrobenzene-1,2-diol) subunit, *i.e.*, tolcapone (**1**), entacapone (**2**), and opicapone (**3**) (Figure 2), are used in clinical practice in association with L-DOPA/AADCi therapy. Their pharmacokinetic properties are quite different from each other and several studies have shown that after systemic administration, tolcapone **1** penetrates into the brain and that the central COMT inhibition observed with **2** is lower and obtained at higher doses, while **3** is only peripherally active^{6,7}. Thus, tolcapone **1** became rapidly the gold standard for COMT inhibition but its high hepatotoxicity led to its withdrawal between 1998 and 2004. It is used today under strict liver enzyme monitoring. The search for new, less toxic COMTIs for PD therapy is of particular interest.

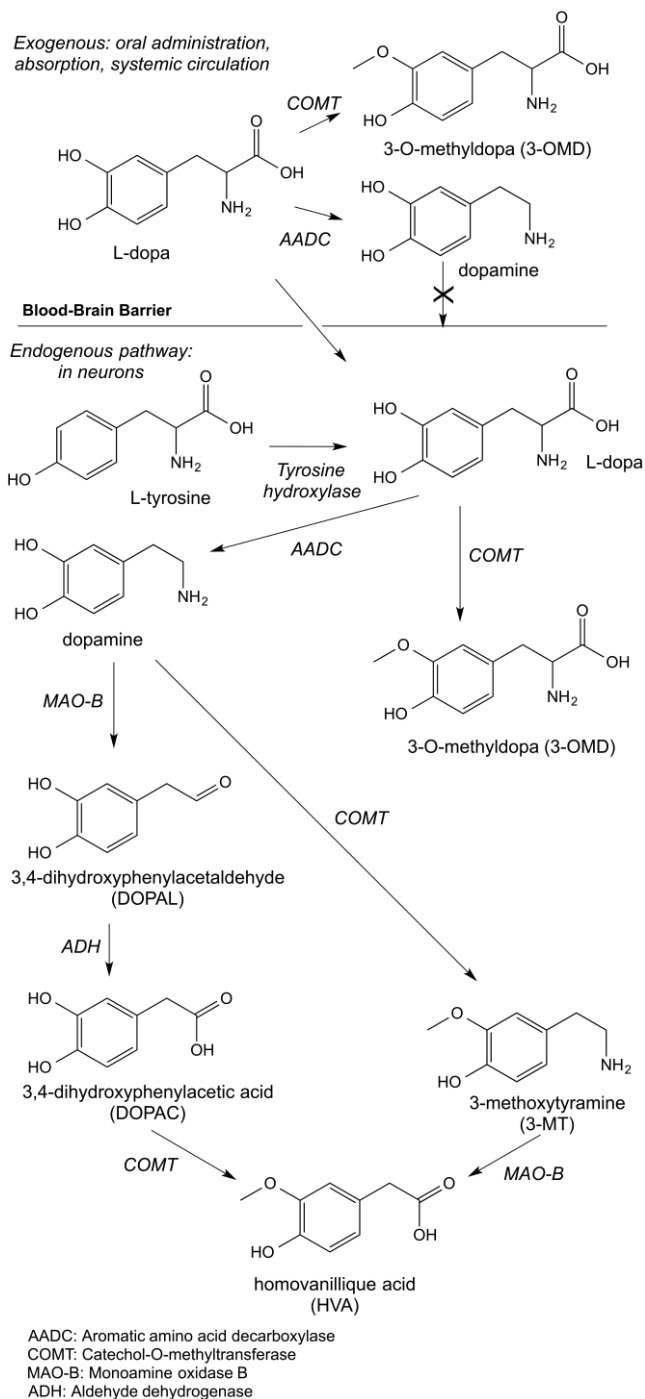


Figure 1. Dopaminergic metabolism.

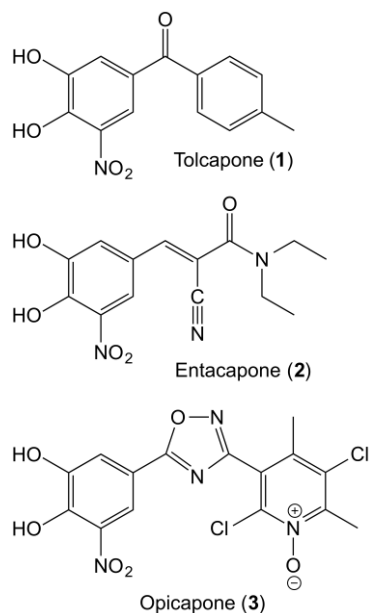


Figure 2. COMTIs currently on the market.

The nematode *Caenorhabditis elegans*, is a non-parasitic soil-dwelling nematode possessing a relatively simple integrated neuronal system^{8,9}. Its neuronal system contains most of the known cellular and molecular components of mammalian brains and constitutes a useful experimental model to study various neurobiological processes^{10,11}. Synaptic communications involving several mammalian neurotransmitters like GABA, acetylcholine, serotonin, dopamine, and glutamate are present in the nematode¹². The dopaminergic neuronal system of *C. elegans* composed of eight neurons is described to play a role in various behaviors like egg-laying, defecation, motor activity, food sensing, and habituation to the touch^{13,14}. This organism has emerged as a valuable *in vivo* model for understanding the basic neurobiological process involved in many human neurological disorders like Alzheimer's disease, PD, Huntington's disease, and prions diseases^{15,16,17,18,19,20,21}. Environmental or experimental neurotoxins exposure like 6-OHDA (6-hydroxydopamine) and MPP⁺ (1-methyl-4-phenylpyridinium), are largely described to induce specific dopaminergic neurodegeneration and is used to develop pharmacological experimental models to study some features of PD^{22,23,24}. These neurotoxins were also used in *C. elegans* to establish pharmacological models to study PD-related neuronal degeneration^{25,26}.

In our research projects towards PD treatments, we became interested in the known *Mucuna pruriens* seeds. Used in the ayurvedic medicine for centuries to treat PD among other ailments, *M. pruriens* seeds have been partly studied. Besides many constituents mentioned in the literature in a recurrent manner but without any sound scientific evidence (serotonin^{27,28}, nicotine²⁷, N,N-dimethyltryptamine, N,N-dimethyltryptamine-N-oxide, bufotenine, 5-methoxy-dimethyltryptamine, 6-hydroxy-1-methyl β -carboline), phytochemical studies have demonstrated the presence of L-DOPA (up to 7%,

preventing their use as food or feed),^{29,30,31,28} two dihydroxylated tetrahydroisoquinoline (diOH-THIQ) derivatives,^{32,33,34,35} along with amino acids,^{34,36,37} lipids,³⁸ flavonoids (but no genistein or genistin²⁸) and triterpenes³⁹. After performing in our laboratories a separation and purification of the seed extract of *M. pruriens*, we characterized a new compound, (1*R*,3*S*)-6,7-dihydroxy-1-methyl-1,2,3,4-

tetrahydroisoquinoline-1,3-dicarboxylic acid (**4**), which shows a dihydroxylated tetrahydroisoquinoline moiety flanked by two carboxylic functions in a *cis* relationship at the 1 and 3 positions and a methyl substituent at position 1.

Given that **4** could derive from L-DOPA after a Pictet-Spengler reaction with pyruvic acid, we synthesized compound **4** and assessed its pharmacological impact on the dopaminergic system and especially the COMT enzyme.

RESULTS

Extraction and isolation of compound **4** from *M. pruriens*

Seed powder of *Mucuna pruriens* was obtained commercially from Banyan Botanicals, Albuquerque, USA with an authenticity certificate from the manufacturer. It has been furthermore identified following the Indian Pharmacopoeia as *M. pruriens* seed powder. Seed powder was extracted by a water-ethanol mixture. Compound **4** isolated by silica gel and reverse phase chromatography and its structure established using HRESIMS, 1D and 2D ¹H-NMR and ¹³C-NMR spectroscopy and polarimetry.

Synthesis of 4. After optimization, we found out that mixing neat L-DOPA and pyruvic acid with trifluoroacetic acid and heating up to 70°C, led to a mixture of two diastereomers in 2:1 ratio (**4**:**4'**). Overnight recrystallization over isopropanol led to the isolation of predominant *cis* isomer **4** with a 94:6 diastereomeric purity in 28% yield (Figure 3).

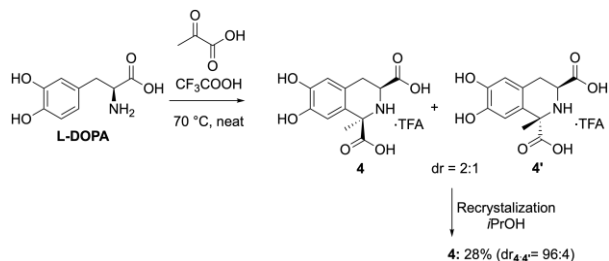


Figure 3. Synthesis of **4**

In vitro studies. We tested compound **4** in a set of in-house enzymatic assays⁴⁰ using cellular lysates, which assessed inhibition of AADC, MAO-B, and COMT, using known inhibitors as controls. Results (see SI) showed that **4** presented a COMT inhibitory activity in the same order of magnitude as tolcapone **1**, together with a negligible inhibitory effect on AADC and MAO-B and low cytotoxicity (See SI).

Compound **4** was also tested for its agonist activity on human D1 and D2L receptors as well as dopamine uptake. At 10 μ M, agonist response of **4** was 0.1 % and - 6.6 % of dopamine response, respectively, with EC_{50} of dopamine being of 71 nM for D1 receptor and 6.7 nM for D2L receptor. The activity of **4** at 10 μ M on dopamine uptake inhibition was - 4.2 % of control (GBR12909) value, the latter showing an IC_{50} of 3.6 nM (See SI). These data show that compound **4** does not compete with dopamine on dopaminergic receptors and dopamine uptake. This suggests a satisfactory selectivity of **4** for COMT, allowing us to further explore the *in vivo* significance of this effect.

In vivo studies: C. elegans model. Wild-type animals N2 strain were used to generate a transgenic line (control^{GFP} line) expressing the *gfp* transgene under the monoamine transporter regulatory sequence (*dat-1p*). As previously described^{41,26} *dat-1p* drove GFP reporter expression in the eight dopaminergic neurons (See SI, Fig. 1A). To generate a *C. elegans* model of dopaminergic injuries, animals were chronically incubated in liquid media with MPP⁺ toxin (1 mM). The deleterious effects of the neurotoxin were evaluated by observation under an epifluorescence microscope of the four anterior dopaminergic neurons class (CEPs) and their associated dendrites (See SI, Fig. 1B). After treatment with MPP⁺ for three days, we observed a significant loss of 41 % of the CEPs neurons and 58 % of their connected dendrites in comparison with the untreated animals (See SI, Fig. 1B, bottom panel). To study the functional impact of the MPP⁺ on dopaminergic neuronal functionality, we used a specific phenotypical test by counting motionless animals in solid media after a short swimming period⁴². The positive control to validate the behavioral test was a dopamine-defective CB1112 line (*cat-2, e1112*) carrying a mutation in the ortholog gene of tyrosine hydroxylase⁴³. We measured an increase of 186 % of motionless animals among MPP⁺ treated animals in comparison with the untreated animals (See SI, Fig. 1C).

A significant improvement of dopaminergic functionality behavior test was observed with treatment with L-DOPA (from 1 up to 3 mM) (Fig. 4A), tolcapone **1** (from 1 up to 1.5 mM) (Fig. 4B), and with compound **4** at solely 1.5 mM (Fig. 4C). These observations suggest that compound **4** may be able to inhibit COMT in *C. elegans*. None of the treatment, however, was able to fully restore motor activity of worms.

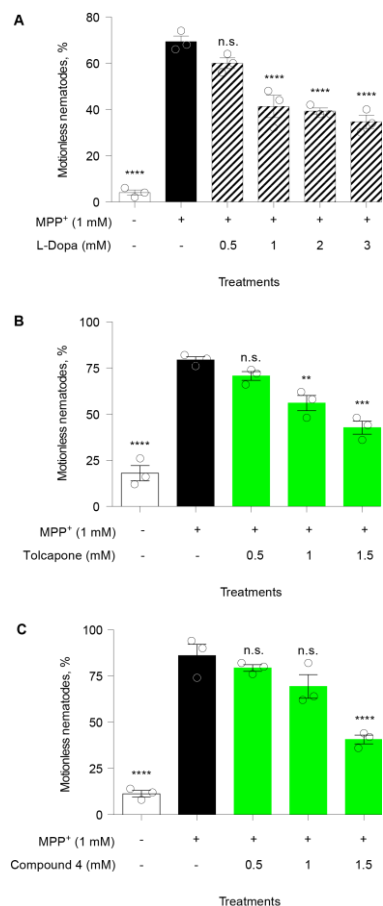


Figure 4. Dysfunctional dopaminergic system induced by MPP⁺ treatment is restored by L-DOPA, tolcapone **1** and **4**. Synchronized L1 stage larvae were incubated in liquid media with MPP⁺ (1 mM) during three days at 20 °C and in presence of various concentration of (A) L-DOPA (0.5, 1, 2 and 3 mM), (B) tolcapone **1** (0.5, 1 and 1.5 mM) and (C) compound **4** (0.5, 1 and 1.5 mM). Locomotion activities after swimming were evaluated with movies analysis produced with a macroscope at low magnification. Data are means \pm s.e.m. of three independent experiments, $n = 150$ animals per experiment and experimental condition. Statistical significance was calculated with a one-way ANOVA followed by a *Dunnett's* multiple comparisons test for the only MPP⁺ treated condition versus all the others experimental conditions; ** $p < 0.01$; *** $p < 0.001$ and **** $p < 0.0001$; n.s., not significant.

During the chronical incubation of MPP⁺, animals were co-treated with L-DOPA (1 mM) and a COMTI (tolcapone **1** or compound **4**, at 1 mM). L-Dopa + tolcapone **1** induced a significant increase (+ 50 %) of the motility of the animals in comparison with the tolcapone **1** untreated L-DOPA condition (Fig. 5A). L-DOPA + **4** induced a significant reduction of 55.5 % of motionless animals in comparison with L-DOPA alone (Fig. 5B). These results suggest that **4** improves the neurobiological dopaminergic restoration observed with L-DOPA in the animals presenting dopaminergic injuries.

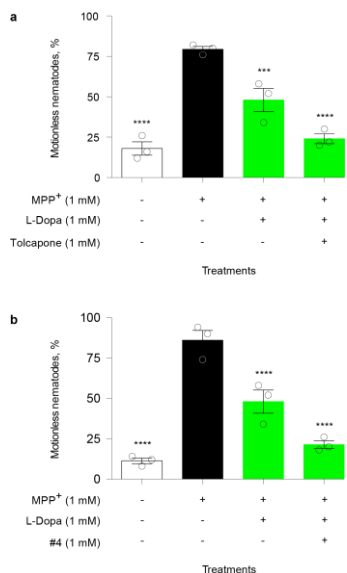


Figure 5. Dopaminergic behavioral effect of L-DOPA administration is enhanced by tolcapone **1** and **4**.

Synchronized L1 stage larvae of control^{GFP} line were chronically incubated in liquid media with MPP⁺ (1 mM) and in presence of L-DOPA (1 mM) during three days at 20 °C. Percentage of motionless animals after a treatment with (A) tolcapone **1** (1 mM) or (B) **4** (1 mM). Data are means ± s.e.m. of three independent experiments, $n = 150$ animals per experiment and experimental condition. Statistical significance was calculated with a one-way ANOVA followed by a *Dunnett's* multiple comparisons test for the only MPP⁺ treated condition versus all the others experimental conditions; *** $p < 0.001$ and **** $p < 0.0001$.

In vivo study: 6-OHDA rat model. We assessed the effect of **4** on a 6-OHDA lesioned rat model, characterized by a unilateral lesion of ascending neurons from the mesencephalon to the striatum. Compound **4** (30 and 100 mg/kg) was compared to (i) saline plus vehicle, (ii) L-DOPA (6 mg/kg) and (iii) L-DOPA (6 mg/kg) plus tolcapone **1** (30 mg/kg) (Figure 6). Over eighteen lesioned rats, six were not further submitted to treatments as they would not display limb hypokinesia. Among the twelve rats submitted to treatments, two were discarded as they would not show any contralateral rotation upon L-DOPA administration. All the ten remaining rats received treatments following a Latin square allocation and a wash-out period of at least three days. Treatments were administered intraperitoneally, so absorption bias did not impact the results.

As expected, L-DOPA induced contralateral rotations, although when L-DOPA was administered alone, its enzymatic degradation limited the intensity of the effect, which was not statistically significant neither on total count nor on the peak intensity of rotations (Figure 6, B and C). When administered along with L-DOPA, tolcapone **1** significantly increased L-DOPA effect, which was of higher intensity and longer duration (Figure 6, A to C). This is due to both the inhibition of plasmatic COMT, which allows more L-DOPA to enter the brain, and the inhibition of central COMT, which allows more L-DOPA

to be transformed into dopamine (See Figure 1). When administered along with L-DOPA, **4** at 30 mg had a similar effect as tolcapone **1**, albeit of a clearly shorter duration (Figure 6, A to C). Also, a 100 mg dose of **4** led to a lower effect than the one observed at 30 mg and was characterized by a wider interindividual variation. This could be rationalized by competition with L-DOPA for its transportation into the brain.

Two hours after the last administration, rats were euthanized and striata were collected for quantification of neuroamines. Neurochemistry has been monitored for dopamine, DOPAC, HVA, 3-OMD, 3-MT, 5-HIAA, and 5-HT on the striatum of each brain hemisphere. Data are in accordance with the model of the mechanism of action of L-DOPA, *i.e.* a crossing of BBB by L-DOPA, which is then down-processed into dopamine and further metabolites. Although this model can be discussed³, the following data interpretation can be made. On the basal healthy striatum, the enzymes of the dopamine pathway (tyrosine hydroxylase, AADC, COMT, and MAO-B) are functioning and a basal, endogenous concentration of L-DOPA, dopamine, DOPAC, HVA, 3-OMD, 3-MT, and NA is observed (See SI, Figure 2). On the basal lesioned striatum, in which dopaminergic neurons have been mostly destroyed, dopamine is very low, as are the concentrations of its metabolites DOPAC, HVA, 3-MT, and NA (See SI, Figure 2). The tyrosine hydroxylase from other neurons (*e.g.*, noradrenergic neurons) remains active³, and produces small amounts of L-DOPA, which is not down-processed by dopaminergic neurons, resulting in a concentration of L-DOPA higher in the lesioned striatum than the one in the healthy striatum. As a result, a slight, non-significant increase of 3-OMD is also seen when compared to healthy striatum, as a result of the remaining activity of COMT (See SI, Figure 2).

Administration of L-DOPA with tolcapone **1** increases the amount of L-DOPA in both healthy and lesioned striatum (Figure 7), suggesting that the central uptake of L-DOPA is efficient but that its central down processing is impaired, either by inhibition of COMT by tolcapone **1** in the healthy striatum or by the lack of dopaminergic neurons in the lesioned striatum. Administration of L-DOPA in combination of **4** does not lead to an increased amount of L-DOPA in the healthy striatum, suggesting that exogenous L-DOPA is down-processed either by AADC and COMT from dopaminergic neurons and that **4** does not inhibit central COMT. In the lesioned striatum, dopaminergic neurons are mostly absent and down-processing L-DOPA is impaired.

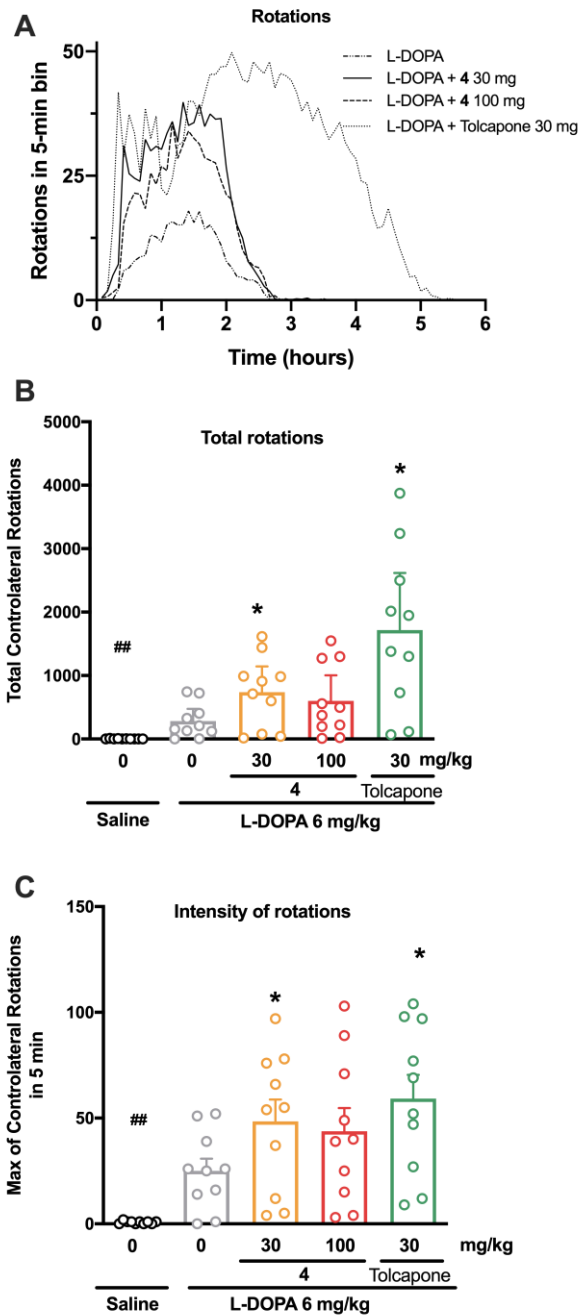


Figure 6. Effect of vehicle, **4** (30 and 100 mg/kg, i.p.) or tolcapone **1** (30 mg/kg, i.p.) in combination with L-DOPA or saline administration on contralateral rotations over 360 min, $n = 10$ rats. A) Rotations in 5 minutes time bin over the duration of the experiment (mean). B) Total rotations over the duration of the experiment (mean). C) Peak number of rotations in any 5 minutes time bin. Bars represent the group mean + 95 % CI; dots represent the individual animal values. Data were analysed by paired t test. * $p < 0.05$, vs Vehicle + L-DOPA. ## $p < 0.05$, L-DOPA vs vehicle + saline.

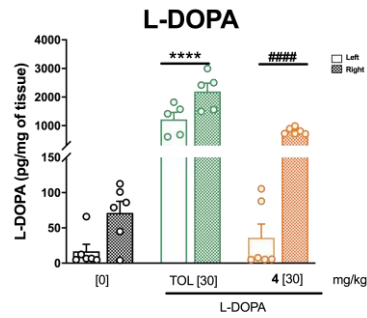


Figure 7: L-DOPA concentration in healthy and lesioned striata after the treatment by tolcapone **1** (30 mg/kg, i.p.) or **4** (30 mg/kg, i.p.) in combination with L-DOPA. Bars represent the group mean; dots represent individual animal values. The data were analysed with a two-way ANOVA ('group' and 'hemisphere' were given as factors) followed by Sidak's multiple comparisons. **** $p < 0.0001$ vs control. #### $p < 0.0001$ vs group L-DOPA + tolcapone **1**.

As tolcapone **1** increases the entry of L-DOPA in the brain, a subsequent increase of the products of AADC and MAO-B, namely dopamine and DOPAC, can be seen in the healthy striatum (Figure 8, A and D). The non-significant increase of NA in this case (Figure 8F) suggests a saturation of the noradrenaline pathway already at the basal level. But as central COMT in the healthy hemisphere is inhibited by tolcapone **1**, HVA, 3-OMD, and 3-MT are not produced as these metabolites imply one step of metabolism by COMT (Figure 8B,C,E). On the lesioned striatum, L-DOPA and tolcapone **1** do not increase the metabolites of L-DOPA, namely dopamine, HVA, 3-OMD, DOPAC or 3-MT (Figure 8A to E). As dopamine is not increased, noradrenaline is not increased either (Figure 8F).

When **4** is administered in combination with L-DOPA, most data strongly suggest that **4** is a peripheral COMT inhibitor, but not a central COMT inhibitor, as the following analysis shows: if not inhibited, COMT from dopaminergic neurons in the healthy hemisphere quickly metabolizes L-DOPA, massively supplied from the blood, into high amounts of 3-OMD (Figure 8C). AADC also metabolizes L-DOPA into dopamine, but as COMT is rather a competing pathway, the increase in dopamine is weaker than the one observed with L-DOPA plus tolcapone **1** (Figure 8A). Dopamine is metabolized by COMT into 3-MT, which is consequently increased as well (Figure 8E). Dopamine is also metabolized by MAO-B into DOPAC which is slightly increased when compared to basal level (Figure 8D), and which is then metabolized by COMT into HVA, also increased compared to basal levels (Figure 8B).

On the lesioned striatum, the COMT from remaining dopaminergic neurons is still able to produce 3-OMD (Figure 8C), but all the other pathways based on the other dopaminergic enzymes are not functional, and there is no increase of dopamine, HVA, DOPAC, 3-MT or noradrenaline (Figure 8A, B, D, E, F) compared to basal state. Data on 5-HT pathway show no effect of **4** on this neurochemical pathway (data not shown).

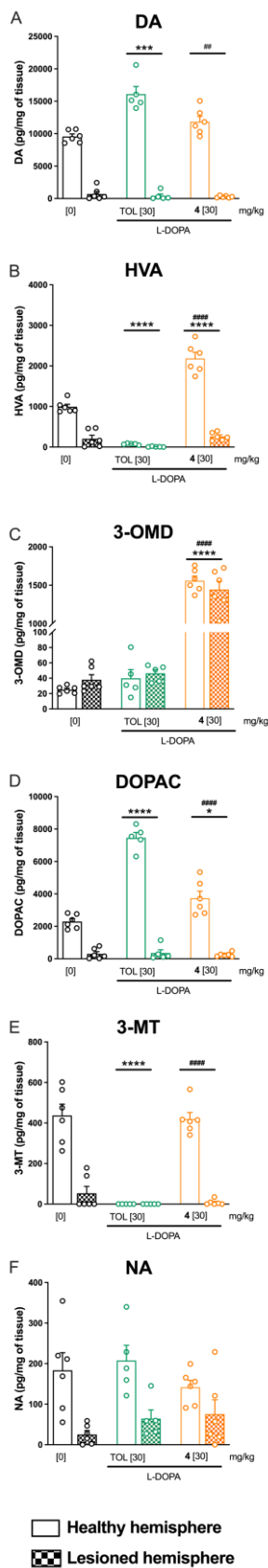


Figure 8. Concentration of L-DOPA metabolites in healthy and lesioned hemisphere after administration of treatments. Data were analyzed with a two-way ANOVA followed by Sidak's multiple comparisons. **** $p < 0.0001$, ** $p < 0.01$ vs control. ##### $p < 0.0001$ vs group L- DOPA + tolcapone **1** (30 mg/kg).

DISCUSSION

These assays on experimental models of PD allow us to validate the *in vivo* effect of COMT inhibitor compound **4** and denote its cooperative molecular impact with L-DOPA to enhance the related dopamine behavior and dopamine concentration.

On the *C. elegans* model, compound **4** showed a significant synergic effect with L-DOPA at an ineffective concentration when alone (1 mM) with a cellular mechanism that remains unclear. Major *C. elegans* behavioral tests used to study the functionality of the dopaminergic neuronal system frequently involve additional neurotransmitters, *e.g.* serotonin implicated for example in the slowing basal response or egg-laying behavior tests¹³. Thus, in the behavioral test that we used⁴², the implication of dopamine in motor activity is not an assay involving *stricto sensu* specifically the dopaminergic system. Nevertheless, we obtained a significant response with the dopamine defective mutant *cat-2* and tolcapone **1**, suggesting that the dopamine system is involved and predominant in the behavioral test used in this study. The neurotoxin MPP⁺ is largely used *in vitro* and *in vivo* to generate pharmacological models of PD^{44,45} including in the *C. elegans* organism²⁵. In contrary of the observation described by Braungart and his collaborators²⁵, our data showed an improvement of the MPP⁺-impaired dopaminergic system by L-DOPA treatment at 1 mM. These observations can be explained by the different experimental setup, including behavioral test and drug administration mode. It also showed that an administration of L-DOPA at 5 mM may induce motionless phenotype with a muscle peripheral effect⁴⁶. In our assays, we did not exceed the concentration of 3 mM of L-DOPA in our experimental condition to avoid these non-neuronal effects.

COMT inhibition of **4**, observed in the *C. elegans* MPP⁺ neurotoxicity model, remains to be more clearly elucidated. Indeed, five orthologs of the human COMTD1 are present in *C. elegans*⁴⁷ and we cannot exclude a divergent affinity of **4** with these various isoforms. In addition, various COMT isoforms present heterogeneity in tissue expression and we focused our investigations only in the dopaminergic system to evaluate the effects of the tested compounds. Yet the reference *in-vivo* rat PD model used in this study corroborates the findings on *C. elegans*, and supports the opinion that the nematode MPP⁺ dopaminergic neuronal loss model can be used for large-scale drug screening approaches in order to identify new active molecular therapeutic compounds, while meeting 3Rs rules pertaining to species replacement²⁵.

The *in-vivo* rat study and associated neurochemistry data strongly suggest that compound **4** does not enter the brain and only inhibits peripheral COMT. Tolcapone **1** is the gold-standard peripheral and central COMT potent inhibitor, with a half-life in rats of 2.9 hours⁶ (1-3 hours in humans⁴⁸). The intensity of the effect of **4** is similar to tolcapone **1**, with no dose-effect relationship and with a duration equal to half of duration of the effect shown by tolcapone **1**. Several hypotheses can be drawn from these data. The intensity of the effect may be limited

to the saturation of enzymatic or transport systems, being either COMT peripheral concentration or L-DOPA BBB transporters, for instance, suggesting that efficient dose determination can only be empirical. Duration of the effect may be related to serum half-life (half-life of **4** is not known at this stage), but also to the peripheral of central nature of the COMT inhibition. Tolcapone **1** being a reversible inhibitor with a IC_{50} of around $0.8 \mu M^{49}$, determination of inhibition constant of **4** with a validated enzymatic assay is warranted.

CONCLUSIONS

The relevance of COMTIs in PD remains timely, as they appear as an efficient treatment of end-of-dose motor fluctuations associated to long-term L-DOPA treatment. The latest marketed COMTI is opicapone **3**, a peripheral, reversible inhibitor whose main interest is to be administered once daily: its half-life is similar to tolcapone **1** but its binding affinity (K_d) is subpicomolar, which translates into a slow complex dissociation rate constant and long duration of action⁵⁰. Tolcapone **1** is the only COMTI that has a central effect. It is still used by patients not responding to peripheral COMTI, despite its significant hepatic toxicity, suggesting the need in the clinic of a safe COMTI acting at the central level. The alleged neurotoxicity of 3-OMD, the L-DOPA metabolite by COMT, also incites to the finding of central COMTIs. But the complexity of the transport of compounds acting on the dopaminergic pathway across the BBB is still to be tamed. The hypothesis of compound **4** being a competitive substrate of COMT, being methylated upon its binding, is still to be explored. The assessment of the toxicity of methylated metabolites of **4** may be of relevance, although the traditional use of *M. pruriens*, which is further validated by this study, has not been associated to specific side-effects. This traditional treatment of PD clearly requires further exploration beyond its significant content in L-DOPA. Nonetheless, at this point, compound **4** can be considered as a promising drug candidate for the development of safe, peripheral COMT inhibitors, useful in the treatment of PD and Lewy bodies disorders.

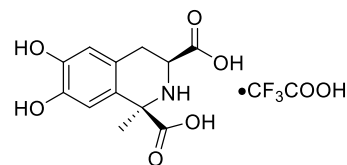
EXPERIMENTAL SECTION

Extraction and isolation of compound **4**

Seed powder of *Mucuna pruriens* was obtained commercially from Banyan Botanicals, Albuquerque, USA with an authenticity certificate from the manufacturer. It has been furthermore identified following the Indian Pharmacopoeia as *M. pruriens* seed powder. The powder (435g) was defatted with acetone (500 ml) by shaking and sonicating for 6 h at room temperature. Defatted material was extracted twice with water-ethanol (1L, 1:1) by shaking and sonicating for 6h. After filtration on paper, filtrate was concentrated (38 g). Crude extract (28 g) was subjected to silica gel column chromatography using solvent systems of increasing polarity: Isopropanol:ethyl acetate (20:19), isopropanol:ethyl acetate:water:acetic acid (20:19:10:1, 20:19:12:1, 20:19:15:1), isopropanol:water:methanol:triethylamine (20:70:5:5).

Fractions were subjected to purification by preparative RP-HPLC using gradient elution with MeOH / 0.2 % TFA in water, from 2 to 25% of MeOH in 25 min. Compound **4** was isolated as a pale greenish amorphous solid. Molecular formula was deduced to be $C_{17}H_{17}NO_6$ from HRESIMS data (m/z 332.113 $[M+H]^+$ (calculated m/z for $C_{17}H_{18}NO_6$: 332.1134). &D and 2D 1H -NMR and ^{13}C -NMR spectra indicated that compound **4** is a 3-carboxy-1-benzyl-3',4',6, 7-tetrahydroxy-1,2,3,4-tetrahydroisoquinoline. The relative configuration of C-1 and C-3 was established by NOESY correlations to be *cis* for the methyl in position 1 and the proton in position 3. $[\alpha]_D^{25}$ value of -44 ($c = 0,25$) suggested that absolute configuration of **4** was (1*S*, 3*S*) as in other tetrahydroisoquinolines isolated previously from *M. pruriens*.

Synthesis of 4. L-DOPA (5 g, 25.3 mmol), pyruvic acid (7 mL, 101.2 mmol) and TFA (2.7 mL, 35.4 mmol) were triturated in a flask and the mixture was heated to 70 °C for about 5 min. High vacuum was then applied to the reaction flask, removing volatiles and forming a homogenous foam, which solidified upon drying. The resulting solid was dissolved with hot *i*PrOH (100 mL), and the solution was cooled down overnight to room temperature. White crystals were collected by filtration, washed with cold 50:50 mixture of *i*PrOH:CH₂Cl₂, then washed with Et₂O. After a drying step, compound **4** was isolated as a white powder (2.67 g, 28 %, **4:4'** = 94:6). Further concentration of the mother liquor followed by precipitation with Et₂O afforded a mixture of compound **4** and **4'** (2.31g, 24%, **4:4'** = 63.5:36.5). $[\alpha]_D^{24} = -44$ ($c = 0.25$, MeOH). 1H NMR (300 MHz, methanol-*d*₄) δ 7.13 (s, 1H), 6.62 (s, 1H), 4.10 (dd, $J = 12.0, 5.3$ Hz, 1H), 3.19 (dd, $J = 16.5, 5.3$ Hz, 2H), 3.10 (dd, $J = 16.5, 12.0$ Hz, 1H), 1.87 (s, 3H). ^{13}C NMR (75 MHz, methanol-*d*₄) δ 173.84, 172.07, 146.95, 146.02, 125.69, 123.37, 115.98, 113.72, 66.09, 53.82, 48.43, 29.94, 24.74. HRMS (ESI⁻): calcd m/z for $[M-H]^-$ $C_{12}H_{12}NO_6$: 266.0665, found: 266.0661.



(1*R*,3*S*)-6,7-dihydroxy-1-methyl-1,2,3,4-tetrahydroisoquinoline-1,3-dicarboxylic acid (**4**)

C. elegans strains, cultures and synchronization of worms. Animals were generally maintained in Petri dishes on solid nematode growth medium (NGM) seeded with OP50 strain of *Escherichia coli* as previously described^{51,52}. Mutant *cat-2* (*e1112*) strain was obtained from the Caenorhabditis Genetics Center (University of Minnesota, St. Paul, MN-USA) and dopaminergic neurons GFP tagged line (*dat-1p::gfp*; NB50)⁵³ was generated by transgenesis technique⁵⁴. For liquid culture media, after hatching, larval stage L1 animals were incubated at 20 °C in liquid S-medium enriched with heat-killed preparation of *E. coli* OP50 strain as a food source. Synchronized animals were prepared by standard bleach method⁵².

Nematode culture and MPP⁺ treatment. Larval stage L1 after hatching were grown in liquid medium during three days at 20 °C under agitation (70 rpm)⁵². For MPP⁺ administration, the neurotoxin was solubilised in water to constitute a 10 mM stock solution and added in culture media at a final concentration of 1 mM.

COMTI and L-DOPA incubation in *C. elegans*. At L4 stage the nematodes were washed off MPP⁺ and culture medium and were incubated for 2 hours with the COMTI (tolcapone **1** and compound **4**, 1 mM) diluted in water containing DMSO 1%. Controls were incubated in the same conditions without COMTI. For L-DOPA treatments, L4 nematodes, after having been washed off MPP⁺ and culture medium, were incubated in S-Basal medium with 1 mM of L-DOPA during 3 hours at 20 °C. For co-administration of L-DOPA and COMTI, worms were incubated during 1 hour at 20 °C with the COMTI, washed with S-basal and treated with L-DOPA during 2 hours at 20 °C.

Neuronal loss assay. Young adult animals expressing the GFP in dopaminergic neuronal system were fixed in PBS 4 % during 15 min at 20 °C and were mounted on fresh 2 % agarose pad slides. The number of CEP (GFP tagged) anterior dopaminergic neurons and their associated dendrites were quantified under an epifluorescence microscope (Zeiss Apotome.2 imaging system) using x63 magnification lens ($n = 50$ animals per experiment and experimental condition with three independent experiments).

Dopaminergic behavioural analysis. To evaluate behaviour, we used a method previously described⁵⁵. Behavioural test was preceded by an incubation of 2 hours in S-basal medium without food source at 20 °C without MPP⁺ in presence or absence of L-DOPA (1 mM) and COMTI. To motivate the movement of the worms, assay plates containing bacteria were prepared by spreading a drop of OP50 *E. coli* in the middle of the plates followed by incubation at 30 °C overnight. A drop of 5 µl of about 10 worms was placed on the assay plate and the assays began 5 min after the drop was absorbed by the agar, *i.e.* at a time where the worms were able to escape and start crawling (recordings were done for 5 min on a dry zone). We performed movies during 1 min (7 fps, Nikon AZ100M microscope) on a total of $n = 50$ worms in triplicate per condition for each experiment (three independent experiments). Crawling velocity was analysed by tracking the centroid of animals by video using the *wrMTrck* plugin of *ImageJ* software⁵⁶. Statistical analysis was performed using *GraphPad Prism 6* (GraphPad Software, La Jolla, CA). Statistical significances of the data were performed using a one-way analysis of variance ANOVA. Multiple corrections were made using post-hoc a *Dunnnett's* test whenever required. $P < 0.05$ was

considered significant. Error bars in figures represent error of the mean (s.e.m).

6-OHDA rat model. To produce neurodegeneration of dopaminergic neurons, 18 male Sprague-Dawley rats received a unilateral intracerebral injection of 6-OHDA by stereotactic delivery. Thirty minutes prior to surgery, animals were given Metacam® (1 mg/kg; s.c) as an analgesic and the noradrenaline uptake inhibitor desipramine (25 mg/kg; i.p.) to protect noradrenergic neurons. Each animal was placed in an anaesthetic chamber supplied with a continuous flow of oxygen (1.5 l/min) and 5% isoflurane. Following loss of consciousness, the animals were installed in a stereotactic frame (Kopf) and maintained under isoflurane during intracerebral injections. Using a glass pipette, each animal was injected 2.5 µl of 6-OHDA solution (5 mg/mL dissolved in sterile water with 0.1 % ascorbic acid) into the right medial forebrain bundle (MFB). The injection site was located according to the following coordinates relative to bregma: - 3.6 mm rostral, 1.6 mm lateral and from -7.5 to -6.5 mm below the dura (Paxinos and Watson, 2007). Twelve animals were selected according to the result of the stepping test performed 3 weeks following the lesion. Only animals displaying limb hypokinesia contralateral to the lesion were used in the efficacy part of the study. Stepping adjustments were measured as described by (Olsson, Nikkhah *et al.* 1995). Forelimb akinesia was assessed as follows. Briefly, the experimenter takes the rat with one hand holding both hindlimbs and the other hand holding one of the forelimbs. The free paw is placed in contact with a flat surface. The experimenter then moves the animal slowly sideways in forehand and backhand directions. The number of adjusting steps is counted for both paws in the backhand and forehand directions.

The effect of **4** followed a within-subject Latin square design (T1 to T4), while tolcapone **1** treatment (T5) was not randomised. The washout period was at least 3 days.

Assessment of rotation was performed as follows. Rotations (*i.e.* net contralateral to the lesion) were assessed for 360 min (0-6 hrs) immediately 30 min after the test item administration using automated rotometers. Rotations were cumulated into successive 5-minute time bins. The following parameters were measured:

- Total rotation was measured by counting the total number of rotations for the duration of the experiment.
- The intensity of rotation was taken as the peak number of contralateral rotations in any 5 minutes time bin.
- The on-time was defined as the sum of 5-minute time bins in which were recorded at least 10 rotations.

For the neurochemistry part, 2 hours after drugs administration, animals were humanely euthanized by anesthetic overdose of Exagon (200 mg/kg) plus Lurocaine (20 mg/kg). Rats unselected for behavioral test after 6-OHDA treatment were euthanized as well. The time of the last compound administration and the exact time of euthanasia were recorded. The brains were quickly removed, placed in an ice-cold glass dish and rapidly

dissected on ice. Both striata were macro-dissected, placed in an Eppendorf tube, frozen on dry ice and stored at -70°C awaiting HPLC analysis. The extent of striatal dopamine depletion as well as the reactivity to the different treatments was assessed by measuring tissue levels of dopamine, 3,4-dihydroxyphenylacetic acid (DOPAC), homovanillic acid (HVA), L-DOPA, 3-O-methyldopa (3-OMD) and 3-methoxytyramine (3-MT) in the striatum, using high-pressure liquid chromatography (HPLC, see below) with an electrochemical detection system. One rat received by mistake compound **4** at 120 mg/kg instead of 30 mg/kg and was not included in the analysis. The day of the biochemical analysis tissues were homogenized in 200 μl of 0.1N HClO_4 , sonicated, and centrifuged at 13,000 rpm for 30 min at 4°C . Aliquots (50 μl) of the supernatants were diluted in HClO_4 (1:4 v/v) before the injection into the HPLC system.

HPLC analysis and electrochemical detection. The tissue concentrations of monoamines were measured by HPLC coupled to the coulometric detection system. The mobile phase of the HPLC system was composed of methanol (7%), NaH_2PO_4 (70 mM), triethylamine (100 $\mu\text{l/l}$), EDTA (0.1 mM), sodium octyl sulphate (100 mg/l) diluted in deionized water (pH 4.2, adjusted with orthophosphoric acid). It was filtered (0.22 μm) before its installation in the system. The mobile phase was delivered through the HPLC column (Hypersil, C18, 150 \times 4.6 mm, particle size 5 μm , C.I.L.) at a flow rate of 1.2 mL/min using an HPLC pump (LC10Ad Vp, Shimadzu, France). The column was protected by a Brownlee-Newgard precolumn (RP-8, 15 \times 3.2 mm, 7 μm ; C.I.L.). The injection of the samples (10 μl) was carried out by a manual injection valve (Rheodyne, model 7725i, C.I.L.) equipped with a loop of 20 μl . The monoamines exit the column at different retention times and passed into the coulometric detection cell (Cell 5014, ESA, Paris, France) equipped with two electrodes. The potential of these two electrodes was fixed *via* the coulometric detector (CoulochemII, ESA, Paris, France) at +350 mV (oxidation) and -270 mV (reduction), respectively. The coulometric detector was connected to a computer through an interface (Ulyss, Azur system, Toulouse, France).

The calibration curves were performed once the peaks in a standard solution (1 ng/10 μl) were well separated in the chromatogram. Calibration curves were performed using three concentrations of DA, DOPAC, L-DOPA, 3-MT, 3-OMD, and HVA injected three times each with an acceptable $r = 0.99$. Standard solutions were used before each series of 10/12 samples to verify the good correspondence of the chromatographic conditions to both the elution time and quantities calculated from the calibration curves. Similarly, the quantities of monoamines in the standards varied according to the brain region investigated. The overall sensitivity for the compounds ranged from 2 pg/10 μl for DA to 30 pg/10 μl for 3-MT with a signal/noise ratio of 3:1. The tissue levels of DA, DOPAC, HVA, L-DOPA, 3-OMD and 3-MT are expressed in pg/mg of tissue.

For behavioral part, statistical analysis was performed using a Paired t-test between Vehicle + Saline (T1) and Vehicle + L-DOPA (T2) treatment. All groups which received L-DOPA were then analyzed with one-way ANOVA followed by Dunnett's *post hoc* test to establish the effect of the compound. For the neurochemistry part, statistical analysis was performed using a Two-way ANOVA ('Group' and 'hemisphere' as given factors) followed by Sidak's multiple comparisons test. All data analysis was performed with *GraphPad Prism 8* (GraphPad Software, La Jolla, CA).

Author information

Corresponding authors

Nicolas Bizat – ICM, Hôpital Pitié Salpêtrière, 47 boulevard de l'Hôpital, 75013 Paris, France; Université de Paris Cité; orcid.org/0000-0001-9643-4417; Email: nicolas.bizat@icm-institute.org

Alexandre Maciuk – Université Paris-Saclay, CNRS, BioCIS, 92290, Châtenay-Malabry, France ; orcid.org/0000-0003-1436-6436 ; Email : alexandre.maciuk@univ-site-paris-saclay.fr

Authors

Valeria Parrales-Macias - ICM, Hôpital Pitié Salpêtrière, 47 boulevard de l'Hôpital, 75013 Paris, France; orcid.org/0000-0003-0967-0468

Abha Harfouche - Université Paris-Saclay, CNRS, BioCIS, 92290, Châtenay-Malabry, France

Laurent Ferrié - Université Paris-Saclay, CNRS, BioCIS, 92290, Châtenay-Malabry, France; orcid.org/0000-0002-1171-205X

Stéphane Haïk - ICM, Hôpital Pitié Salpêtrière, 47 boulevard de l'Hôpital, 75013 Paris, France; orcid.org/0000-0001-6022-1188

Patrick P. Michel - ICM, Hôpital Pitié Salpêtrière, 47 boulevard de l'Hôpital, 75013 Paris, France

Rita Raisman-Vozari - ICM, Hôpital Pitié Salpêtrière, 47 boulevard de l'Hôpital, 75013 Paris, France; orcid.org/0000-0003-4873-3935

Bruno Figadère – Université Paris-Saclay, CNRS, BioCIS, 92290, Châtenay-Malabry, France; orcid.org/0000-0003-4226-8489

Author contribution

|| V.P.-M. and A.H. contributed equally to the work. V.P.-M.: investigation. A.H.: investigation. S.H.: resources. P.P.M.: conceptualization. R.R.V.: conceptualization and funding acquisition. B.F.: conceptualization, supervision, writing – review & editing. N.B.: conceptualization, funding acquisition, investigation, methodology, visualization, formal analysis, writing – original draft. A.M.: conceptualization, funding acquisition, methodology, project administration, visualization, writing – original draft.

Funding

This work was supported by a CARNOT grant. A.H. was supported by Ministry of Higher Education of Syria (N° 1034).

Notes

The authors declare no competing financial interest. We thank the *Caenorhabditis Genetics Center* for provided strains. We acknowledge the technical service from the *Brain Institute* platforms in particular: David Akbar (*Celis*); Dominique Langui, Aymeric Millecamps, Claire Lovo and Basile Gurchenkov (icm.Quant); Annick Prigent (Histomic). MOTAC is acknowledged for 6-OHDA rat model experiments.

Abbreviations

PD, Parkinson's Disease; COMT, catechol-O-methyltransferase; L-DOPA, L-3,4-dihydroxyphenylalanine; MPP⁺, 1-methyl-4-phenylpyridinium; 6-OHDA, 6-hydroxydopamine; *C. elegans*, *Caenorhabditis elegans*; SNC, *substantia nigra pars compacta*; AADC, aromatic amino acid decarboxylase inhibitor; 3-OMD, 3-O-methyl dopa; AADC, aromatic amino acid decarboxylase; MAO-B, Monoamine Oxidase-B; DOPAL, 3,4-Dihydroxyphenylacetaldehyde; DOPAC, 3,4-Dihydroxyphenylacetic acid; 3-MT, 3-Methoxytyramine; HVA, Homovanillic acid; ADH, Aldehyde Dehydrogenase; diOH-THIQ, dihydroxylated tetrahydroisoquinoline; BBB, Blood Brain Barrier; IC₅₀, half maximal inhibitory concentration; HPLC high-pressure liquid chromatography.

Supporting Information. Results for COMT, AADC and MAO-B inhibition assay, dopaminergic receptors and transporter binding assay and cytotoxicity assay. DA cell loss model using MPP⁺ in the nematode *C. elegans*. NMR spectral data for isolated and synthesized compound 4.

References

- (1) Müller, T. Pharmacokinetics and Pharmacodynamics of Levodopa/Carbidopa Cotherapies for Parkinson's Disease. *Expert Opin. Drug Metab. Toxicol.* **2020**, *16* (5), 403–414. <https://doi.org/10.1080/17425255.2020.1750596>.
- (2) Panneton, W. M.; Kumar, V. B.; Gan, Q.; Burke, W. J.; Galvin, J. E. The Neurotoxicity of DOPAL: Behavioral and Stereological Evidence for Its Role in Parkinson Disease Pathogenesis. *PLoS ONE* **2010**, *5* (12), e15251. <https://doi.org/10.1371/journal.pone.0015251>.
- (3) Chagraoui, A.; Boulain, M.; Juvin, L.; Anouar, Y.; Barrière, G.; Deurwaerdère, P. L-DOPA in Parkinson's Disease: Looking at the "False" Neurotransmitters and Their Meaning. *Int. J. Mol. Sci.* **2019**, *21* (1), 294. <https://doi.org/10.3390/ijms21010294>.
- (4) Sotnikova, T. D.; Beaulieu, J.-M.; Espinoza, S.; Masri, B.; Zhang, X.; Salahpour, A.; Barak, L. S.; Caron, M. G.; Gainetdinov, R. R. The Dopamine Metabolite 3-Methoxytyramine Is a Neuromodulator. *PLoS ONE* **2010**, *5* (10), e13452. <https://doi.org/10.1371/journal.pone.0013452>.
- (5) Lee, E.-S. Y.; Chen, H.; King, J.; Charlton, C. The Role of 3-O-Methyl dopa in the Side Effects of l-Dopa. *Neurochem. Res.* **2008**, *33* (3), 401–411. <https://doi.org/10.1007/s11064-007-9442-6>.
- (6) Forsberg, M. Pharmacokinetics and Pharmacodynamics of Entacapone and Tolcapone after Acute and Repeated Administration: A Comparative Study in the Rat. *J. Pharmacol. Exp. Ther.* **2003**, *304* (2), 498–506. <https://doi.org/10.1124/jpet.102.042846>.
- (7) Fabbri, M.; Ferreira, J. J.; Lees, A.; Stocchi, F.; Poewe, W.; Tolosa, E.; Rascol, O. Opicapone for the Treatment of Parkinson's Disease: A Review of a New Licensed Medicine: Opicapone in The Treatment of PD. *Mov. Disord.* **2018**, *33* (10), 1528–1539. <https://doi.org/10.1002/mds.27475>.
- (8) Dougherty, E. C. The Genera and Species of the Subfamily Rhabditinae Micoletzky, 1922 (Nematoda): A Nomenclatorial Analysis, Including an Addendum on the Composition of the Family Rhabditidae Orley, 1880. *J. Helminthol.* **1955**, *29* (3), 105–152.
- (9) RF White; Van Tol, H. The Structure of the Ventral Nerve Cord of *Caenorhabditis elegans*. *Philos. Trans. R. Soc. Lond. B Biol. Sci.* **1976**, *275* (938), 327–348. <https://doi.org/10.1098/rstb.1976.0086>.
- (10) Bargmann, C. I. Neurobiology of the *Caenorhabditis elegans* Genome. *Science* **1998**, *282* (5396), 2028–2033. <https://doi.org/10.1126/science.282.5396.2028>.
- (11) Hodgkin, J.; Herman, R. K. Changing Styles in *C. elegans* Genetics. *Trends Genet.* **1998**, *14* (9), 352–357. [https://doi.org/10.1016/S0168-9525\(98\)01543-1](https://doi.org/10.1016/S0168-9525(98)01543-1).
- (12) Hobert, O. The Neuronal Genome of *Caenorhabditis elegans*. *WormBook* **2013**, 1–106. <https://doi.org/10.1895/wormbook.1.161.1>.
- (13) McDonald, P. W.; Jessen, T.; Field, J. R.; Blakely, R. D. Dopamine Signaling Architecture in *Caenorhabditis elegans*. *Cell. Mol. Neurobiol.* **2006**, *26* (4–6), 591–616. <https://doi.org/10.1007/s10571-006-9003-6>.
- (14) Sulston, J.; Dew, M.; Brenner, S. Dopaminergic Neurons in the Nematode *Caenorhabditis elegans*. *J. Comp. Neurol.* **1975**, *163* (2), 215–226. <https://doi.org/10.1002/cne.901630207>.
- (15) Alexander, A. G.; Marfil, V.; Li, C. Use of *Caenorhabditis elegans* as a Model to Study Alzheimer's Disease and Other Neurodegenerative Diseases.

- Front. Genet.* **2014**, *5*.
<https://doi.org/10.3389/fgene.2014.00279>.
- (16) Bessa, C.; Maciel, P.; Rodrigues, A. J. Using *C. elegans* to Decipher the Cellular and Molecular Mechanisms Underlying Neurodevelopmental Disorders. *Mol. Neurobiol.* **2013**, *48* (3), 465–489. <https://doi.org/10.1007/s12035-013-8434-6>.
- (17) Bizat, N.; Peyrin, J. M.; Haik, S.; Cochois, V.; Beaudry, P.; Laplanche, J. L.; Neri, C. Neuron Dysfunction Is Induced by Prion Protein with an Insertional Mutation via a Fyn Kinase and Reversed by Sirtuin Activation in *Caenorhabditis elegans*. *J. Neurosci.* **2010**, *30* (15), 5394–5403. <https://doi.org/10.1523/JNEUROSCI.5831-09.2010>.
- (18) Dexter, P. M.; Caldwell, K. A.; Caldwell, G. A. A Predictable Worm: Application of *Caenorhabditis elegans* for Mechanistic Investigation of Movement Disorders. *Neurotherapeutics* **2012**, *9* (2), 393–404. <https://doi.org/10.1007/s13311-012-0109-x>.
- (19) Hannan, S. B.; Dräger, N. M.; Rasse, T. M.; Voigt, A.; Jahn, T. R. Cellular and Molecular Modifier Pathways in Tauopathies: The Big Picture from Screening Invertebrate Models. *J. Neurochem.* **2016**, *137* (1), 12–25. <https://doi.org/10.1111/jnc.13532>.
- (20) Harrington, A. J.; Yacoubian, T. A.; Slone, S. R.; Caldwell, K. A.; Caldwell, G. A. Functional Analysis of VPS41-Mediated Neuroprotection in *Caenorhabditis elegans* and Mammalian Models of Parkinson's Disease. *J. Neurosci.* **2012**, *32* (6), 2142–2153. <https://doi.org/10.1523/JNEUROSCI.2606-11.2012>.
- (21) Vashlishan, A. B.; Madison, J. M.; Dybbs, M.; Bai, J.; Sieburth, D.; Ch'ng, Q.; Tavazoie, M.; Kaplan, J. M. An RNAi Screen Identifies Genes That Regulate GABA Synapses. *Neuron* **2008**, *58* (3), 346–361. <https://doi.org/10.1016/j.neuron.2008.02.019>.
- (22) Dauer, W.; Przedborski, S. Parkinson's Disease: Mechanisms and Models. *Neuron* **2003**, *39* (6), 889–909. [https://doi.org/10.1016/S0896-6273\(03\)00568-3](https://doi.org/10.1016/S0896-6273(03)00568-3).
- (23) Glinka, Y.; Gassen, M.; Youdim, M. B. H. Mechanism of 6-Hydroxydopamine Neurotoxicity. In *Advances in Research on Neurodegeneration*; Riederer, P., Calne, D. B., Horowski, R., Mizuno, Y., Poewe, W., Youdim, M. B. H., Eds.; Journal of Neural Transmission. Supplementa; Springer Vienna: Vienna, 1997; Vol. 50, pp 55–66. https://doi.org/10.1007/978-3-7091-6842-4_7.
- (24) Przedborski, S.; Jackson-Lewis, V. Mechanisms of MPTP Toxicity. *Mov. Disord. Off. J. Mov. Disord. Soc.* **1998**, *13 Suppl 1*, 35–38.
- (25) Braungart, E.; Gerlach, M.; Riederer, P.; Baumeister, R.; Hoener, M. C. *Caenorhabditis elegans* MPP⁺ Model of Parkinson's Disease for High-Throughput Drug Screenings. *Neurodegener. Dis.* **2004**, *1* (4–5), 175–183. <https://doi.org/10.1159/000080983>.
- (26) Nass, R.; Hall, D. H.; Miller, D. M.; Blakely, R. D. Neurotoxin-Induced Degeneration of Dopamine Neurons in *Caenorhabditis elegans*. *Proc. Natl. Acad. Sci.* **2002**, *99* (5), 3264–3269. <https://doi.org/10.1073/pnas.042497999>.
- (27) Contin, M.; Lopane, G.; Passini, A.; Poli, F.; Iannello, C.; Guarino, M. *Mucuna pruriens* in Parkinson Disease: A Kinetic-Dynamic Comparison With Levodopa Standard Formulations. *Clin. Neuropharmacol.* **2015**, *38* (5), 201–203. <https://doi.org/10.1097/WNF.000000000000098>.
- (28) Cassani, E.; Cilia, R.; Laguna, J.; Barichella, M.; Contin, M.; Cereda, E.; Isaias, I. U.; Sparvoli, F.; Akpalu, A.; Budu, K. O.; Scarpa, M. T.; Pezzoli, G. *Mucuna pruriens* for Parkinson's Disease: Low-Cost Preparation Method, Laboratory Measures and Pharmacokinetics Profile. *J. Neurol. Sci.* **2016**, *365*, 175–180. <https://doi.org/10.1016/j.jns.2016.04.001>.
- (29) Pugalenti, M.; Vadivel, V.; Siddhuraju, P. Alternative Food/Feed Perspectives of an Underutilized Legume *Mucuna pruriens* Var. Utilis—A Review. *Plant Foods Hum. Nutr.* **2005**, *60* (4), 201–218. <https://doi.org/10.1007/s11130-005-8620-4>.
- (30) Raina, A. P.; Tomar, J. B.; Dutta, M. Variability in *Mucuna pruriens* L. Germplasm for L-Dopa, an Anti Parkinsonian Agent. *Genet. Resour. Crop Evol.* **2012**, *59* (6), 1207–1212. <https://doi.org/10.1007/s10722-012-9836-4>.
- (31) Fernandez-Pastor, I.; Luque-Muñoz, A.; Rivas, F.; Medina-O'Donnell, M.; Martinez, A.; Gonzalez-Maldonado, R.; Haidour, A.; Parra, A. Quantitative NMR Analysis of L-Dopa in Seeds from Two Varieties of *Mucuna pruriens*. *Phytochem. Anal.* **2019**, *30* (1), 89–94. <https://doi.org/10.1002/pca.2793>.
- (32) Amarasekera, A. S.; Jansz, F. R. Studies on *Mucuna* Species of Sri Lanka. II. Determination of the Tetrahydroisoquinoline Content of Seeds. *J. Natl. Sci. Found. Sri Lanka* **8** (2), 99–103.
- (33) Kumar, P.; Rawat, A.; Keshari, A. K.; Singh, A. K.; Maity, S.; De, A.; Samanta, A.; Saha, S. Antiproliferative Effect of Isolated Isoquinoline Alkaloid from *Mucuna pruriens* Seeds in Hepatic Carcinoma Cells. *Nat. Prod. Res.* **2016**, *30* (4), 460–463. <https://doi.org/10.1080/14786419.2015.1020489>.
- (34) Misra, L.; Wagner, H. Alkaloidal Constituents of *Mucuna pruriens* Seeds. *Phytochemistry* **2004**, *65* (18), 2565–2567. <https://doi.org/10.1016/j.phytochem.2004.08.045>.
- (35) Siddhuraju, P.; Becker, K. Rapid Reversed-Phase High Performance Liquid Chromatographic Method for the Quantification of L-Dopa (L-3,4-Dihydroxyphenylalanine), Non-Methylated and Methylated Tetrahydroisoquinoline Compounds from *Mucuna* Beans. *Food Chem.* **2001**, *6*.
- (36) Siddhuraju, P.; Vijayakumari, K.; Janardhanan, K. Chemical Composition and Protein Quality of the Little-Known Legume, Velvet Bean (*Mucuna pruriens* (L.) DC.). *J. Agric. Food Chem.* **1996**, *44* (9), 2636–2641. <https://doi.org/10.1021/jf950776x>.
- (37) Misra, L.; Wagner, H. Extraction of Bioactive Principles from *Mucuna pruriens* Seeds. *Indian J. Biochem. Biophys.* **2007**, *44*, 5.
- (38) Misra, L.; Wagner, H. Lipid Derivatives from

- (39) Khan, M. Y.; Kumar, V. Mechanism of Antihypertensive Effect of *Mucuna pruriens* L. Seed Extract and Its Isolated Compounds. *J. Complement. Integr. Med.* **2017**, *14* (4).
<https://doi.org/10.1515/jcim-2017-0014>.
- (40) Harfouche, A.; Alata, W.; Leblanc, K.; Figadère, B.; Maciuk, A. Label-Free LC/HRMS-Based Enzymatic Activity Assay for the Detection of DDC, MAO and COMT Inhibitors. *J. Pharm. Biomed. Anal.* **2022**, *212*, 114598.
- (41) Lynch, A. S.; Briggs, D.; Hope, I. A. Developmental Expression Pattern Screen for Genes Predicted in the *C. elegans* Genome Sequencing Project. *Nat. Genet.* **1995**, *11* (3), 309–313.
<https://doi.org/10.1038/ng1195-309>.
- (42) Vidal-Gadea, A.; Topper, S.; Young, L.; Crisp, A.; Kressin, L.; Elbel, E.; Maples, T.; Brauner, M.; Erbguth, K.; Axelrod, A.; Gottschalk, A.; Siegel, D.; Pierce-Shimomura, J. T. *Caenorhabditis elegans* Selects Distinct Crawling and Swimming Gaits via Dopamine and Serotonin. *Proc. Natl. Acad. Sci.* **2011**, *108* (42), 17504–17509.
<https://doi.org/10.1073/pnas.1108673108>.
- (43) Lints, R.; Emmons, S. W. Patterning of Dopaminergic Neurotransmitter Identity among *Caenorhabditis elegans* Ray Sensory Neurons by a TGFbeta Family Signaling Pathway and a Hox Gene. *Dev. Camb. Engl.* **1999**, *126* (24), 5819–5831.
- (44) Langston, J. W. The MPTP Story. *J. Park. Dis.* **2017**, *7* (s1), S11–S19.
<https://doi.org/10.3233/JPD-179006>.
- (45) Martinez, T. N.; Greenamyre, J. T. Toxin Models of Mitochondrial Dysfunction in Parkinson's Disease. *Antioxid. Redox Signal.* **2012**, *16* (9), 920–934. <https://doi.org/10.1089/ars.2011.4033>.
- (46) Wintle, R. F.; Van Tol, H. H. M. Dopamine Signaling in *Caenorhabditis elegans*—Potential for Parkinsonism Research. *Parkinsonism Relat. Disord.* **2001**, *7* (3), 177–183.
[https://doi.org/10.1016/S1353-8020\(00\)00055-9](https://doi.org/10.1016/S1353-8020(00)00055-9).
- (47) Hobert, O. Neurogenesis in the Nematode *Caenorhabditis elegans*. *WormBook* **2010**.
<https://doi.org/10.1895/wormbook.1.12.2>.
- (48) Dingemans, J.; Jorga, K. M.; Schmitt, M.; Gieschke, R.; Fotteler, B.; Zürcher, G.; Prada, M.; van Brummelen, P. Integrated Pharmacokinetics and Pharmacodynamics of the Novel Catechol-O-Methyltransferase Inhibitor Tolcapone during First Administration to Humans. *Clin. Pharmacol. Ther.* **1995**, *57* (5), 508–517.
[https://doi.org/10.1016/0009-9236\(95\)90035-7](https://doi.org/10.1016/0009-9236(95)90035-7).
- (49) De Santi, C.; Giulianotti, P. C.; Pietrabissa, A.; Mosca, F.; Pacifici, G. M. Catechol-O-Methyltransferase: Variation in Enzyme Activity and Inhibition by Entacapone and Tolcapone. *Eur. J. Clin. Pharmacol.* **1998**, *54* (3), 215–219.
<https://doi.org/10.1007/s002280050448>.
- (50) St. Onge, E.; Vanderhoof, M.; Miller, S. Ongentys (Opicapone): A New COMT Inhibitor for the Treatment of Parkinson's Disease. *Ann. Pharmacother.* **2020**, 106002802097456.
<https://doi.org/10.1177/1060028020974560>.
- (51) Brenner, S. The Genetics of *Caenorhabditis elegans*. *Genetics* **1974**, *77* (1), 71–94.
- (52) Stiernagle, T. Maintenance of *C. elegans*. *WormBook* **2006**. <https://doi.org/10.1895/wormbook.1.101.1>.
- (53) Dominguez-Meijide, A.; Parrales, V.; Vasili, E.; González-Lizárraga, F.; König, A.; Lázaro, D. F.; Lannuzel, A.; Haik, S.; Del Bel, E.; Chehín, R.; Raisman-Vozari, R.; Michel, P. P.; Bizat, N.; Outeiro, T. F. Doxycycline Inhibits α -Synuclein-Associated Pathologies *in Vitro* and *in Vivo*. *Neurobiol. Dis.* **2021**, *151*, 105256.
<https://doi.org/10.1016/j.nbd.2021.105256>.
- (54) Mello, C.; Fire, A. Chapter 19 DNA Transformation. In *Methods in Cell Biology*; Elsevier, 1995; Vol. 48, pp 451–482.
[https://doi.org/10.1016/S0091-679X\(08\)61399-0](https://doi.org/10.1016/S0091-679X(08)61399-0).
- (55) Vidal-Gadea, A. G.; Pierce-Shimomura, J. T. Conserved Role of Dopamine in the Modulation of Behavior. *Commun. Integr. Biol.* **2012**, *5* (5), 440–447. <https://doi.org/10.4161/cib.20978>.
- (56) Nussbaum-Krammer, C. I.; Neto, M. F.; Brielmann, R. M.; Pedersen, J. S.; Morimoto, R. I. Investigating the Spreading and Toxicity of Prion-like Proteins Using the Metazoan Model Organism *C. Elegans*. *J. Vis. Exp.* **2015**, No. 95, 52321.
<https://doi.org/10.3791/52321>.